DYNA
http://dyna.medellin.unal.edu.co/

UNIVERSIDAD NACIONAL DE COLOMBIA

First-principles calculations of the structural and electronics properties of YInN alloy

G. Patricia Abdel Rahim-Garzón [a], Jairo Arbey Rodríguez-Martínez [b], María Guadalupe Moreno-Armenta [c] & Miguel José Espitia-Rico[d]

[a] Facultad Tecnológica, Universidad Distrital Francisco José de Caldas, Bogotá, Colombia. ggabdelr@unal.edu.co,
[b] Universidad Nacional de Colombia, sede Bogotá, Facultad de Física, Bogotá, Colombia. jarodriguezm@unal.edu.co
[c] Centro de Nanociencias y Nanotecnología, Universidad Nacional Autónoma de México, Ensenada, Mexico. aeoaun25@gmail.com
[d] Facultad Ingeniería, Universidad Distrital Francisco José de Caldas, Bogotá, Colombia. miguelespitiarico@yahoo.com

Received: June 17th, 2020. Received in revised form: February 4th, 2021. Accepted: February 22th, 2021.

Abstract
We study the structural and electronic properties of $Y_xIn_{1-x}N$ in the concentrations x = 0, ¼, ½, ¾, and 1 in the B1, B2, B3, and B4 structures. The calculations show that for $Y_{0.75}In_{0.25}N$, the B1 structure is the most energetically favorable. It was determined that between $0 < x < \sim 0.12$ in the $(1 \times 1 \times 2)$ supercell, the most energetically stable structure is the B3 phase. Additionally, between $\sim 0.12 < x < \sim 0.6$ concentrations x of yttrium, the compound is most energetically favorable in the B4 phase. Technical data that are in agreement with these results were recently reported by other authors. Finally, between $0.6 \sim < x < 1$, the most stable phase is B1. Additionally, there is no phase transition between the four structures considered. The DOS and band structure showed that $Y_{0.75}In_{0.25}N$ in the B1 and B3 phases exhibits semiconductor behavior, with a direct gap of ~0.6 eV and ~0.7 eV, respectively, while $Y_{0.75}In_{0.25}N$ in the B4 phase has an indirect one of ~0.8 eV.

Keywords: DFT; $Y_xIn_{1-x}N$; supercell: semiconductor; energy gap.

Cálculo en primeros principios de las propiedades estructurales y electrónicas de la aleación YInN

Resumen
Hemos estudiado las propiedades estructurales y electrónicas del $Y_xIn_{1-x}N$ en las concentraciones x = 0, ¼, ½, ¾, y 1 en las estructuras B1, B2, B3 y B4. Los calculos mostraron que para el $Y_{0.75}In_{0.25}N$ en la estructura B1 el compuesto es energéticamente mas favorable. Se determinó que entre $0 < x < \sim 0.12$ en la supercelda de $(1 \times 1 \times 2)$ la estructura mas estable energéticamente es la fase B3. Adicionalmente entre $\sim 0.12 < x < \sim 0.6$ concentraciones x de Ytrio el compuesto es mas favorable energéticamente en la fase B4 y finalmente entre $\sim 0.6 < x < 1$ la fase mas estable es la B1. Adicionlamente se hallo que no existe transiciones de fase en las cuatro estructuras consideradas. La DOS y la estructura de bandas muestra que $Y_{0.75}In_{0.25}N$ en las fases B1 y B3 presentan un comportamiento semiconductor con un gap de ~0.6 eV and ~0.7 eV, respectivamente mientras que $Y_{0.75}In_{0.25}N$ en la fase B4 tiene un gap indirecto de ~0.8 eV.

Palabras clave: DFT; YInN; supercelda; semiconductor; gap de energía.

1. Introduction

In recent years, new materials that exhibit electronic and optical properties that are modulated by various parameters have been developed. In this context, $Y_xIn_{1-x}N$ is a material that is potentially attractive for industry, because it is made up of two materials, InN and YN, which exhibit very different behavioral characteristics under external hydrostatic pressure: the optical gap of InN increases with increasing pressure, while that of YN decreases [1]. Thus, it

How to cite: Abdel Rahim-Garzón, G.P., Rodríguez-Martínez, J.A., Moreno-Armenta, M.G. and Espitia-Rico, M.J., First-principles calculations of the structural and electronics properties of YInN alloy.. DYNA, 88(217), pp. 50-57, April - June, 2021.

is to be expected that for certain concentrations of yttrium, the optical gap would be constant upon varying the pressure. This behavior would be useful in devices that work under highly variable pressure. The nitride group III-V is based on the first transition metals, which possess physical properties of a high degree of electron mobility, high degree of hardness, low fragility, stability at high temperatures, high melting point, and good thermal and electrical conductivity, which implies a potential for use in the development of optoelectronic devices, devices for magnetic storage, hard coatings for cutting tools, and protection against corrosion [1,7,8,17].

In a previous study, Abdel Rahim Garzón, G. P. [1,8] found that in its ground state the crystallization and lattice parameters for YN is B1, with ~4.91 Å, and for InN it is B4, with ~3.58 Å. The bulk moduli are B_0, ~163 GPa and B_0, ~119 GPa, respectively, and the volume increases as the compound has more *d* valence electrons and a greater presence of electrons in the inner layers, so we can reasonably assume that the natural crystallization phase for $Y_xIn_{1-x}N$ will be between these two phases. Abdel Rahim Garzón, G. P. and Jairo Arbey Rodríguez Martínez [8,9], using DFT, studied the structural and electronic properties of the compound YInN in the B2 and B1 phases, with concentrations *x* of ¼, ½, and ¾ of Y. It was found that in the B1 phase, at a concentration of ¾ yttrium (Y) the material behaves as a semiconductor, while in the B2 phase it is metallic at the three concentrations. The cohesion energy decreases with increasing Y concentration, and this is observed for both phases, and the gap energy depends on the yttrium concentration.

They found that for the compound $Y_{0.5}In_{0.5}N$, the ground state is B4, with a difference of energies between the minima of the structures B1 and B4 of ~0.025 eV/unit formula, with a possible B4 to B1 phase transition of the structure at a pressure of P_T ~1.36 GPa. In the band structure, it was observed that at P=0 in the B1 phase there is a metallic behavior, and in the B4 phase and in the phase transition from the semiconductor to the metal phase an indirect semiconductor behavior is exhibited [8,10]. Additionally, they studied the compound YIn_3N_4 in the B1 and B4 phases and found that the base state of the crystallization for this compound is B4, with a possible phase transition of the structure from B4 to B1 with a pressure of P_T ~5.6 GPa. The B1 phase exhibits metallic behavior, while the B4 phase is a semiconductor with a gap energy of ~0.2 eV [8,11].

Zoita et al. [13] reported on the synthesis of $Y_xIn_{1-x}N$ with low levels of Y ($x < 0.1$), experimentally determining that the base state is WZ, and on increasing the melting point of the material, the lattice constant increases and the bandwidth increases linearly towards blue. Also, they determined that the base state of YN is the B1 phase, with an indirect energy gap of ~0.498eV. Tholander et al. [2] report that the composition of thin films with Y (content up to x=0.5) depends on the lattice parameters, and using ab initio calculations they determined that the $Y_xIn_{1-x}N$ wurtzite phase is the lowest in energy among the relevant alloy structures for $0 < x \leq 0.5$. Additionally, it was determined that this compound used as films on AlN not only reduces surface roughness but also improves the crystalline quality. Also, the piezoelectric properties of YInN were improved, converting it into a possible candidate for future electroacoustic applications. In addition, in a theoretical study by N. Benyounes et al. [5], YN was suggested as a possible alloy for tuning the direct and indirect bandgap in metastable zincblende (B3) InN.

In the present paper, the NaCl-type (B1), CsCl-type (B2), ZnS-type (B3), and WZ-type (B4) phases of $Y_xIn_{1-x}N$ are studied as first step for a later study in which it will be determined in which phase the compound is energetically more stable or metastable, and the potential changes of phase will be investigated. Also, a detailed study of its structural stability in the four phases is presented. Plots of energy vs. volume at T = 0K are shown, and some thermodynamic and structural properties are determined, such as the volume unit, $B = -V(\partial P/\partial V)_T$, its derivative, the cohesive energy, and the unit cell volume. With respect to the electronic structure, a detailed analysis is made of the densities of state (DOS), and the band structure is plotted in order to determine the behavior of the direct and indirect bandgap. This article is organized as follows: First, the method that is used is described; in the following section, a study of the stability and the electronic properties is presented for YN, InN, and $Y_xIn_{1-x}N$; and last, a summary is presented, along with some conclusions with respect to $Y_xIn_{1-x}N$.

2. Computational methods

The calculations were performed using density functional theory (DFT), with the full potential linearized augmented plane wave (FP-LAPW) method, as implemented in wien2k code [14]. The exchange and correlation effects are dealt with by using the generalized gradient approximation (GGA) with Perdew–Burke–Ernzerhof parametrization [15]. For all concentrations of *x,* the Y parameters are: Y: muffin-tin radius = 1.8 u.a., In; muffin-tin radius = 1.85 u.a, and N: muffin-tin radius = 1.6 u.a, in addition to other values used, such as: l_{max}= 10.0. l_{max} is the factor that determines the maximum value of *l*. R_{kmax} = 8.0, R_{kmax} determines the size for the base of φ_k functions and is equal to $R_{kmax}=R_{mt}\times K_{max}$, where K_{max} is the magnitude of the largest *G* vector, and R_m is the muffin-tin radius of the smallest sphere. The energy of separation between the shell and the valence states is -8.0 Ry. Total number of 0.25 vectors in the first Brillouin zone is *k* = 1000 for all phases. Convergence criterion in the energy of the self-consistent cycles is 0.0001 Ry. For calculating the structural, electronic, and magnetic properties of YN, InN, and $Y_xIn_{1-x}N$, a $(1 \times 1 \times 2)$ supercell with 8 atoms was used. Furthermore, Wien2K revealed a tetragonal structure.

3. Results and discussion

3.1 Structural properties of InN, YN, and $Y_xIn_{1-x}N$

In Tables 1 and 2, the optimized structural parameters are shown, such as: lattice constant (a), ratio (c/a), bulk modulus (B0), and cohesion energy minimum (E0), listed for the YN and InN compounds in the NaCl, CsCl, zincblende, and wurtzite structures, labeled B1, B2, B3, and B4, respectively. Some values of the structural parameters obtained are compared with theoretical and experimental data available in the literature [16–21].

Table 1 shows the calculations carried out in this investigation and by other authors for YN in the four phases, where the B1 (NaCl) phase and the B4 (WZ) phase are the most energetically favorable structures in the $1 \times 1 \times 2$ geometry of YN. They fit well to the theoretical data reported by other authors [16,17]. In Table 2, the data for InN can be seen in the $1 \times 1 \times 2$ geometry, calculated in this investigation and by other authors using the $1 \times 1 \times 1$ geometry, where it can be seen that the most stable phase is B3 (ZnS phase), with an energy $\sim 0.24\ eV$ higher than the metastable B4 phase (WZ phase) [18–21]. Additionally, for InN in the B4 phase, the lattice parameter, the ratio of c/a, and the modulus of volume are in excellent agreement with the experimental data, ~1.69%, ~0.43 %, and ~3.27 %, respectively.

Table 1.
The structural parameters of **YN** in the B1, B2, B3, and B4 structures. Total energies and volumes are given per unit cell (containing 8 atoms). The parameter $a_0(\text{Å})$ in B1, B2, and B3 is taken as $a(\text{Å}) = a_0(\text{Å})/\sqrt{2}$ where $a(\text{Å})$ is the lattice constant

	a[Å]	$\frac{c}{2a}$	V[Å^3]	B [Gpa]	E_{min}[eV]
B1	3.47 3.49 [16]	$\sqrt{2}$ $\sqrt{2}$ [16]	29.61	156 131.9[16]	-12.95
B2	3.00	$\sqrt{2}$	27.04	141	-11.14
B3	3.73	$\sqrt{2}$	36.88	111	-12.46
B4	3.75 3.78 [17]	1.602 1.576[17]	36.74	114 110.3[17]	-12.64

Source: The Authors

Table 2.
Structural parameters of **InN** in the B1, B2, B3, and B4 structures. Total energies and volumes are given per unit cell (containing 8 atoms). The parameter $a_0(\text{Å})$ in B1, B2, and B3 is taken as $a(\text{Å}) = a_0(\text{Å})/\sqrt{2}$, where $a_0(\text{Å})$ is the lattice constant

	a[Å]	$\frac{c}{2a}$	V[Å^3]	B [Gpa]	E_{min}[eV]
B1	3.33	$\sqrt{2}$	26.11	153	-5.54
B2	2.98	$\sqrt{2}$	26.51	115	-3.68
B3	3.57	$\sqrt{2}$	32.21	120	-5.94
B4	3.59 3.53 [18] 3.52[19] 3.53[Exp-20]	1.62 1.615 [18] 1.612[19] 1.613[Exp-20]	32.13	122 126[Exp-21]	-5.70

Source: The Authors

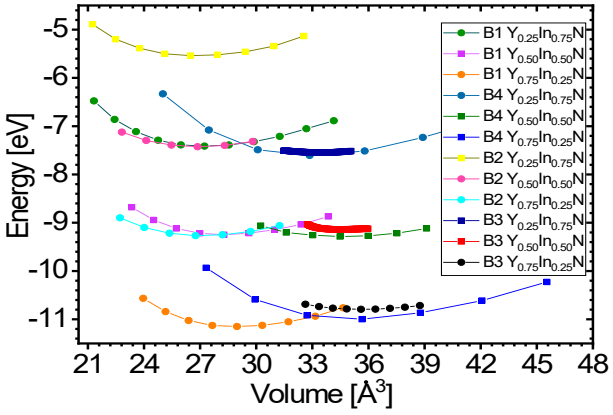

Figure 1. Energy vs. volume for the compound YInN
Source: The Authors

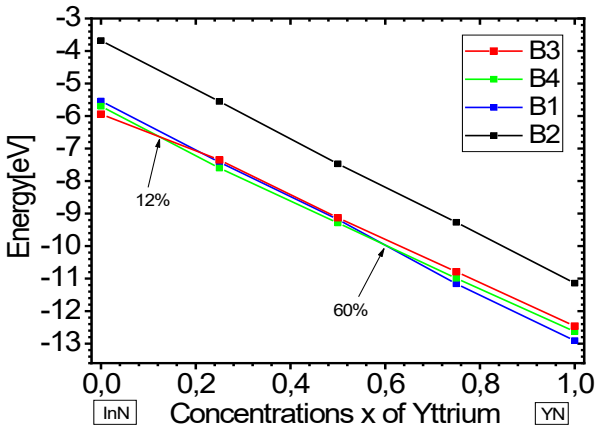

Figure 2. Energy vs. concentrations x of yttrium
Source: The Authors

Fig. 1 shows the cohesion energy-volume curves corresponding to the B1, B2, B3, and B4 structures for the different concentrations x of Y atoms considered in this paper. All total energy-volume curves have a parabola-like behavior and were fit to the Murnaghan equation of state [22] in order to determine their ground state properties. In Tables 3 and 4, the structural parameter of $Y_xIn_{1-x}N$ at the concentrations x = ¼, ½, and ¾ are listed for each of the B1, B2, B3, and B4 structures. It can be seen in Fig. 1 and Table 3 that for the $Y_{0.75}In_{0.25}N$ compound, the B1 structure has a minimum total energy value of $\sim -11.16\ eV/mol$, so it can be considered to be the most energetically stable, with differences with respect to the B4, B3, and B2 structures. The least energetically favorable one is the B2 structure, with the highest energy difference with respect to the B1 structure. For $Y_{0.75}In_{0.25}N$, the B4 structure is the most favorable, with a minimum energy of $\sim -0.99 eV/mol$, followed by the B1 structure, with an energy difference of $\sim 0.17 eV/mol$.

Table 3.
The structural parameters of $Y_xIn_{1-x}N$ in the B1, B2, B3, and B4 structures. Total energies and volumes are given per unit cell (containing 8 atoms). The parameter $a_0(\text{Å})$ in B1, B2, and B3 is taken as $a(\text{Å}) = a_0(\text{Å})/\sqrt{2}$, where $a(\text{Å})$ is the lattice constant, $c/2a = \sqrt{2}$

	B1 [8,9]			
	a_{min} [Å]	V[Å^3]	B [Gpa]	E_{min}[eV]
$Y_{0.25}In_{0.75}N$ [11]	3.38	27.26	145	-7.42
$Y_{0.50}In_{0.50}N$ [10]	3.42	28.16	147	-9.18
$Y_{0.75}In_{0.25}N$	3.45	29	159	-11.16
	B2 [8]			
	a_{min} [Å]	V[Å^3]	B [Gpa]	E_{min}[eV]
$Y_{0.25}In_{0.75}N$	2.991	26.76	134	-5.55
$Y_{0.50}In_{0.50}N$	2.994	26.84	128	-7.47
$Y_{0.75}In_{0.25}N$	3.004	27.11	129	-9.27
	B3			
	a_{min} [Å]	V[Å^3]	B [Gpa]	E_{min}[eV]
$Y_{0.25}In_{0.75}N$	3.62	33.44	118	-7.35
$Y_{0.50}In_{0.50}N$	3.66	34.63	109	-9.14
$Y_{0.75}In_{0.25}N$	3.69	35.65	108	-10.79

Source: The Authors

Table 4.
Structural parameters of $Y_xIn_{1-x}N$ in the B4 structure. Total energies and volumes are given per unit cell (containing 8 atoms), where u_1(YN) = 0.396 and u_2(InN)=0.389

	B4 [8]				
	a_{min} [Å]	$\frac{c}{2a}$	V[Å^3]	B [Gpa]	E_{min}[eV]
$Y_{0.25}In_{0.75}N$ [11]	3.65	1.56	32.90	135	-7.60
$Y_{0.50}In_{0.50}N$ [10]	3.71	1.57	34.53	121	-9.29
$Y_{0.75}In_{0.25}N$	3.72	1.58	35.20	123	-10.99

Source: The Authors

Finally, for the $Y_{0.75}In_{0.25}N$ compound, the B3 structure is the most favorable one, with a total energy minimum value of $\sim -10.79\ eV/mol$, followed by the B1 structure, with an energy difference of $\sim 0.37 eV/mol$. (Table 4).

Fig.2 shows the variation in total energy vs. the concentration x of Y, and there it can be seen that for concentrations from $x = 0$ to ~ 0.12, the B3 structure has the lowest energy, and at this point B4 crosses its path, becoming the most stable up to about ~ 0.6, where B1 becomes more stable. These results are in good agreement with previously-reported theoretical and experimental data [2]. They indicate that the YInN compound, as it approaches both ends, adopts the ground structures of the binary compounds B1-B4, belonging to InN and YN.

In Fig. 3, we plot the lattice parameter versus x concentration of Y atoms in the B1, B2, B3, and B4 structures considered in this study. This variation in the four phases is significant and nonlinear, with a downward bowing. The bowing parameters are negative and small: $b_{aB2} \sim -0.01486$ Å, $b_{aB1} \sim -0.08$Å, $b_{aB3} \sim -0.034$Å, and $b_{aB4} \sim -0.125$Å, as can be seen in Table 5. These small values are coherent with the usual assumption that there should be a relative lattice matching in the four phases between the YN and InN binary compounds that causes some strain. This strain may be due to a decrease in the ionic bond length between the cations and the anions as the yttrium replaces indium on the cationic site. Indeed, the cation-anion bond length decrease is usually attributed to the smaller ionic yttrium radius. This suggests that there is a kind of nonlinear charge distribution transferability as the more covalent In-N bond is replaced by a Y-N bond with a more ionic character.

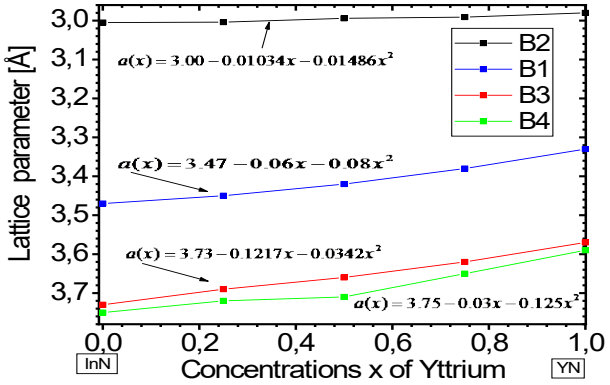

Figure 3. Lattice parameter vs. concentrations x of yttrium
Source: The Authors

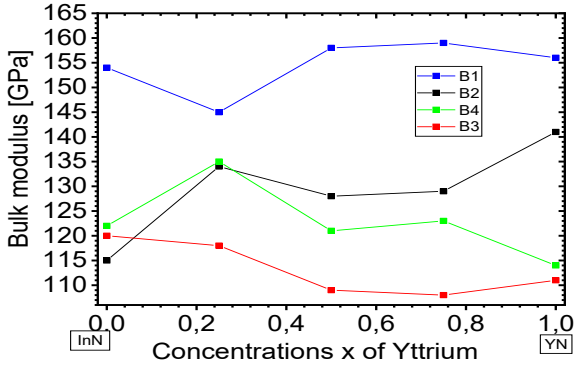

Figure 4. Bulk modulus vs. concentrations x of yttrium
Source: The Authors

In Fig. 4, it is shown that the bulk modulus decreases in the B1 and B4 phases for values $x \geq \sim 0.5$ of yttrium, and in the B2 and B3 phases it increases for values $x \geq \sim 0.5$ of yttrium. Furthermore, between $0 \leq x \leq \sim 0.25$ of yttrium, the bulk modulus decreases in the B1and B4 phases. Also, there is an increase in the B4 and B2 phases, between $\sim 0.5 \leq x \leq 1$ of yttrium.

3.2 Phase Transition

It can be seen in Fig.1 that for the $Y_{0.50}In_{0.50}N$ compound there is an intersection between the energy-volume curves between the most favorable state, B4, and the B1 state, because there is a phase transition from B4 to B1 caused by pressure [10]. In order to calculate the transition pressure at the cutoff point of Fig. 5, the value of the derivative was graphically calculated at the cutoff point in order to find the value of the transition pressure.

Table 5.
Bowing parameters

Phase	Lattices parameter versus x concentration in $Y_xIn_{1-x}N$
B2	$a(x) = 3 - 0.01034x - 0.01486x^2$
B1	$a(x) = 3.47 - 0.06x - 0.08x^2$
B3	$a(x) = 3.73 - 0.1217x - 0.034x^2$
B4	$a(x) = 3.75 - 0.03x - 0.125x^2$

Source: The Authors

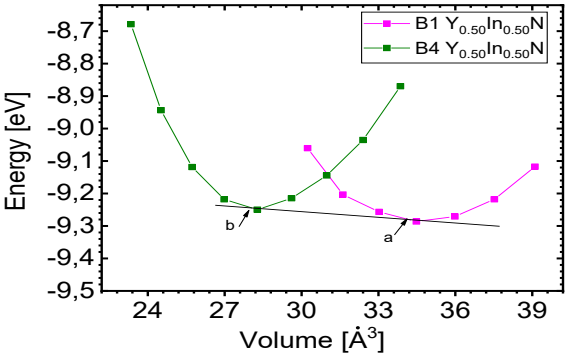

Figure 5. Energy vs. volume for the compound YInN
Source: The Authors

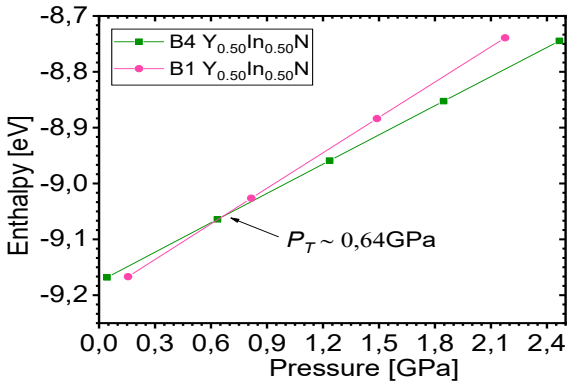

Figure 6. Enthalpy vs. pressure for the compound YInN
Source: The Authors

First, a straight line was drawn that passes through the cutoff point, trying to make it pass through some points of the curves, as shown in Fig. 5, where point (a) indicates $Y_{0.50}In_{0.50}N$ in the B1 phase in the conditions near and before the transition from $Y_{0.50}In_{0.50}N$ in the B4 phase, $P > P_T$, and point (b) indicates $Y_{0.50}In_{0.50}N$ in the B4 phase in conditions near and after the phase transition to $Y_{0.50}In_{0.50}N$ in the B1 phase, $P < P_T$. The value of the transition pressure also can be seen more precisely in Fig. 6, where the transition $Y_{0.50}In_{0.50}N$ in the B1 phase to $Y_{0.50}In_{0.50}N$ in the B4 phase is shown. It is predicted that this transition occurs for $P_T \sim 0{,}64GPa$; at this pressure, the enthalpies of the two structures are the same.

In the next section, we study the electronic properties of $Y_{0.50}In_{0.50}N$ at the points that are marked in Fig. 5. It is important to determine the electronic properties of this material in its different phases and different volumes in order to study the response of the behavior under pressure. This response is determined by the changes in the distances to first neighbors and changes in symmetry, which are related to the band structure.

3.3 Electronic properties of YInN

In Figs. 7–12, the results are presented for the density of states (DOS) (partial and total) and the band structures for the most stable compound, $Y_{0.75}In_{0.25}N$ in the B1, B4, and B3 phases, respectively. In all the figures, we take the Fermi level as the zero energy.

The DOS in Figs. 7–9 shows that the compound exhibits a semiconductor behavior in all three phases. We note that in the valence of the region under $\sim -10\ eV$, there are two very high peaks, where their greatest contribution is N-2*s* and In-4*d*, and below the Fermi level there exists another peak, where the greatest contribution is from the orbitals N-2*p*, with small contributions from In-5*s*. Finally, an energy gap is found at $\sim 0.6eV$ in the B1 phase and another at $\sim 0.8eV$ in the B4 phase, while for $Y_{0.75}In_{0.25}N$ in the B3 phase, it can be seen that in the valence region under $\sim -10.84eV$, there are two very high peaks where the greatest contribution is from N-2*s*, and below the Fermi level there are three peaks where the greatest contributions are from orbitals N-2*p,* In-5s, and In-4*d*, and finally an energy gap of $\sim 0.7eV$ is noted.

Figs. 10–12 show the band structure of $Y_{0.75}In_{0.25}N$ in the B1, B4, and B3 phases, respectively. From the band structures, Figs. 10–12, we found the same three regions observed in the DOS; in all three, we found a semiconductor band gap. For the B1 phase, there is a direct gap at the Γ point, the B4 has an indirect gap located between the maximum point M in the valence band and the minimum point Γ in the conduction band, and finally the B3 phase has a direct gap located at the Γ point. Finally, Figs. 13–14 and Figs. 15–16 show the DOS and band structure of $Y_{0.50}In_{0.50}N$ in the B1 and B4 phases, respectively. The DOS and the band structure were calculated from points immediately before and after the transition point. In these figures, it can be seen that there are no changes in its structure compared with $Y_{0.75}In_{0.25}N$ in the B1 and B4 phases in Figs. 7–8 and Figs. 10–11. This is because the transition pressure is very small.

4. Conclusions

We have studied the structural and electronic properties of the $Y_xIn_{1-x}N$ compound in the B1, B2, B3, and B4 structures for concentrations of x = 0, ¼, ½, ¾, and 1 with a $1 \times 1 \times 2$ geometry, where it was found that these compounds can coexist at a temperature of $T = 0K$. The calculations showed that the $Y_{0.75}In_{0.25}N$ structure in the B1 phase is the most energetically favorable. N. Benyounes et al. suggest that the alloy YInN in the metastable B3 phase allows carrying out the synchronization of the energy gap [5]. In the present investigation, it was found that for the compound in the $1 \times 1 \times 2$ geometrical structure between $0 < x < (\sim 0.12)$ x of yttrium, the most stable phase is B3, and a metastable phase in the B4 phase was found with a maximum energy of $\sim 0.24\ eV$. Furthermore, our calculations show that between $\sim 0.12 < x < \sim 0.6$ this compound is more energetically stable in the B4 phase, which is in agreement with that reported by other authors [2]. Finally, it was found that between $\sim 0.6 < x < 1$, the compound is the most stable in the B1 structure, as indicated in previous reports. For the $Y_{0.75}In_{0.25}N$ compound, there is no phase transition between the B2, B3, and B4 structures. We studied the DOS and band structure for the $Y_{0.75}In_{0.25}N$ compound and found that it exhibits a semiconductor behavior, an indirect band gap in the B4 structure, and a direct band gap in the B1 and B3 structures. Finally, for the $Y_{0.50}In_{0.50}N$ compound there is a phase transition from the B4 to the B1 structure, with a volume reduction of ~21% at a transition pressure of ~0.64 GPa. The study of the DOS and band structure for $Y_{0.50}In_{0.50}N$ in the B4 and B1 structures around the points of transition shows no change in the band gap width.

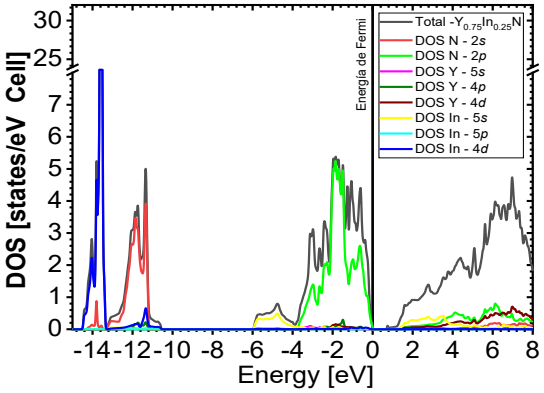

Figure 7. DOS partial and total for $Y_{0.75}In_{0.25}N$ in the B1 structure at P=0
Source: The Authors

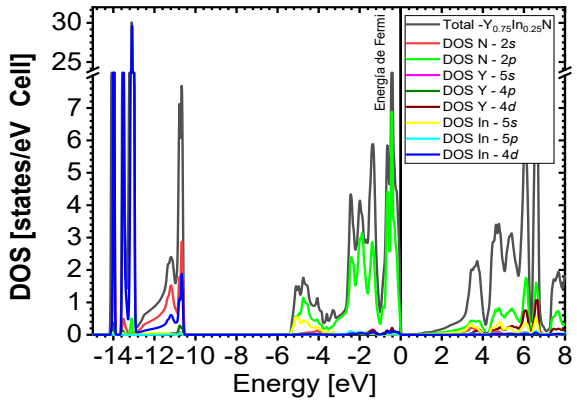

Figure 8. DOS partial and total for $Y_{0.75}In_{0.25}N$ in the B4 structure at P=0
Source: The Authors

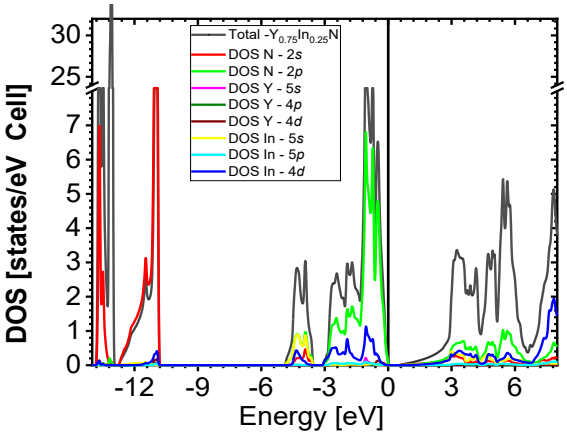

Figure 9. DOS partial and total for $Y_{0.75}In_{0.25}N$ in the B3 structure at P=0
Source: The Authors

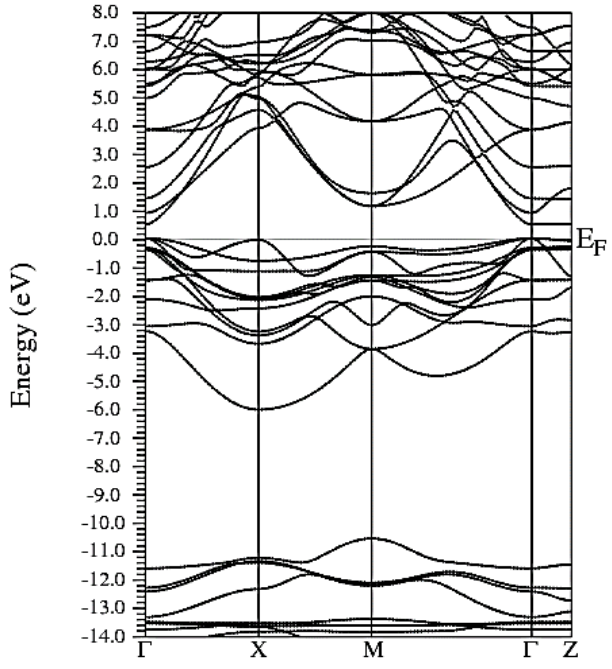

Figure 10. Electronic bands of $Y_{0.75}In_{0.25}N$ with B1-like structure at P=0
Source: The Authors

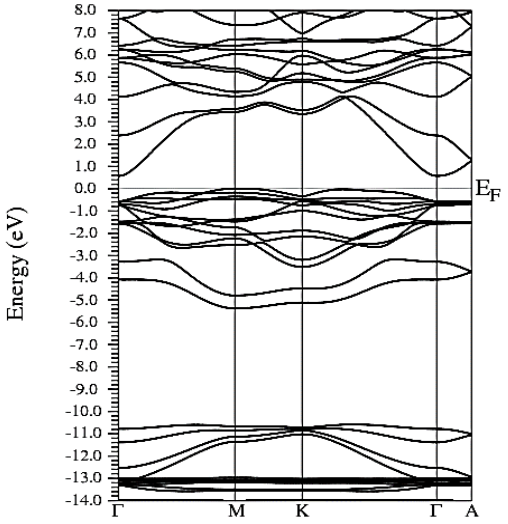

Figure 11. Electronic bands of $Y_{0.75}In_{0.25}N$ with B4-like structure at P=0
Source: The Authors

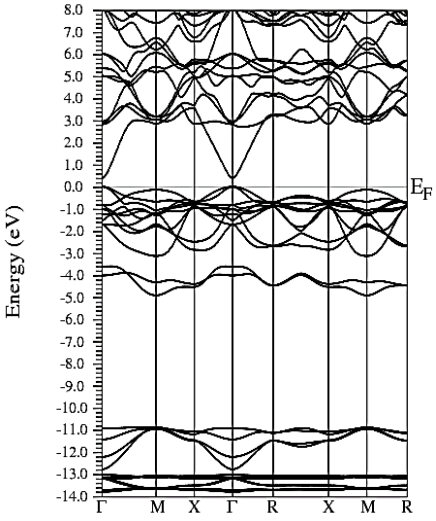

Figure 12. Electronic bands of $Y_{0.75}In_{0.25}N$ in the B3 structure at P=0
Source: The Authors

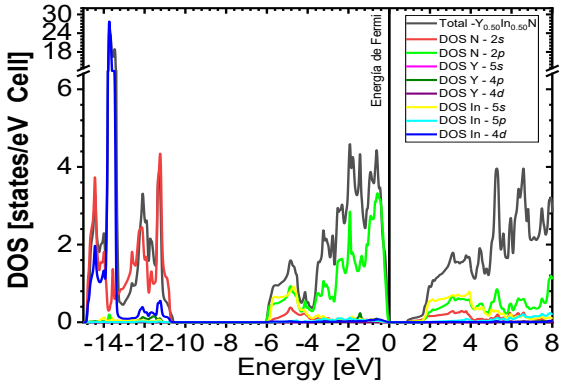

Figure 13. DOS partial and total for $Y_{0.50}In_{0.50}N$ in the B1 before of the phase transition to $Y_{0.50}In_{0.50}N$ in the B4.
Source: The Authors

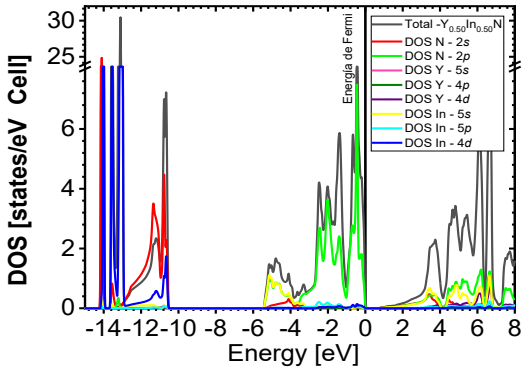

Figure 14. DOS partial and total for $Y_{0.50}In_{0.50}N$ in the B4 after of the phase transition $Y_{0.50}In_{0.50}N$ in the B1.
Source: The Authors

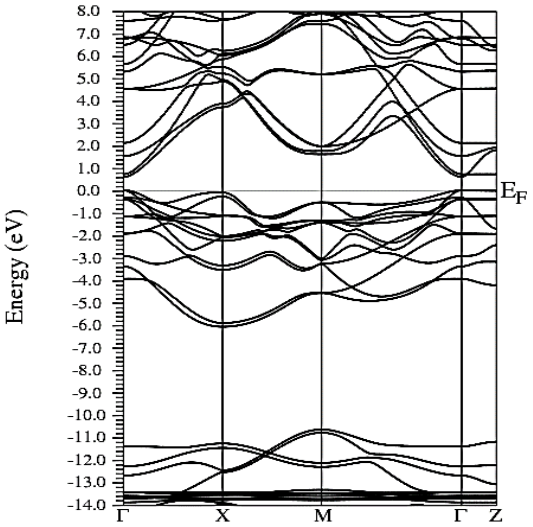

Figure 15. Electronic bands for $Y_{0.50}In_{0.50}N$ in the B1 before of the phase transition to $Y_{0.50}In_{0.50}N$ in the B4.
Source: The Authors

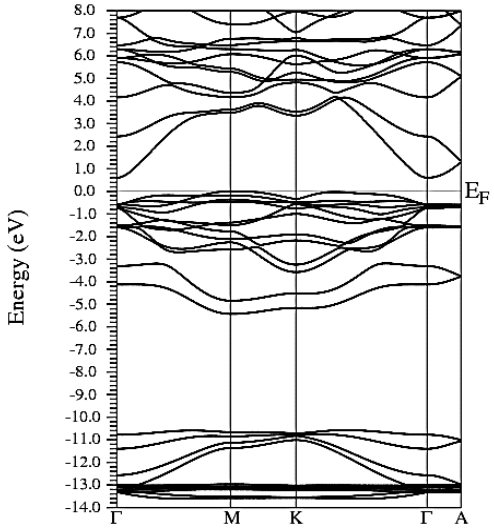

Figure 16. Electronic bands for $Y_{0.50}In_{0.50}N$ in the B4 after of the phase transition $Y_{0.50}In_{0.50}N$ in the B1.
Source: The Authors

References

[1] Mancera, L., Rodríguez, J.A. and Takeuchi, N.. Theoretical study of the stability of wurtzite, zinc-blende, NaCl and CsCl phases in group IIIB and IIIA nitrides. Phys. stat. sol. (b), 241, pp. 2424-2428, 2004. DOI: 10.1002/pssb.200404910

[2] Tholander, C., Birch, J., Tasnádi, F., Hultman, L., Palisaitis, J., Persson, P.O.Å., Jensen, J., Sandström, P., Alling, B. and Žukauskaitė, A., Ab initio calculations and experimental study of piezoelectric $Y_xIn_{1-x}N$ thin films deposited using reactive magnetron sputter epitaxy, Acta Materialia, 105, pp. 199-206, 2016. DOI: 10.1016/j.actamat.2015.11.050

[3] K-Maurya, T., Kumar, S. and Auluck, S., Ab-initio study of electronic and optical properties of InN in wurtzite and cubic phases, Optics Communications, 283, pp. 4655-4661, 2010. DOI: 10.1016/j.optcom.2010.07.011

[4] Xu ,Y.-N. and Ching, W.Y., Electronic, optical and structural properties of some wurtzite crystals, Phys. Rev. B, 48, pp. 4335-4350, 1993.

[5] Benyounes, N. and Boucenna, M., Band structure and related electronic properties of $Y_xIn_{1-x}N$ ternary system, Superlattices and Microstructures 75, pp. 144-150, 2014. DOI: 10.1016/j.spmi.2014.07.009

[6] Gueddim, A., Bouarissa, N., Gacem, L. and Villesuzanne, A., Structural phase stability, elastic parameters and thermal properties of YN from first-principles calculation, Chinese Journal of Physics, 56(5), pp. 1816-1825, 2018. DOI: 10.1016/j.cjph.2018.08.014

[7] Lakdja, A., Bouhafs, B. and Ruterana, P., Ordering effects on the electronic structures of AlN/GaN, InN/GaN and InN/AlN superlattices, Computational Materials Science, 33(1), pp. 157-162, 2005. DOI: 10.1016/j.commatsci.2004.12.054

[8] Abdel Rahim-Garzón, G.P, Estudio ab initio dela estabilidad del compuesto YInN, MSc. Thesis, Department of Physical, Universidad Nacional de Colombia, Bogotá, Colombia, 2006.

[9] Abdel Rahim-Garzón, G.P y Rodríguez-Martínez, J.A., Estudio ab-initio de la estabilidad del compuesto YInN en las fases CsCl Y NaCl, Revista Colombiana de Física, [en línea]. 38(3), pp. 1054-1057, 2006. Disponible en: https://dialnet.unirioja.es/servlet/articulo?codigo=2286763

[10] Abdel Rahim-Garzón, G.P. y Rodríguez-Martínez, J.A., Análisis mediante primeros principios de las propiedades estructurales y electrónicas y las transiciones de fase wurtzita a NaCl el compuesto $Y_{0.5}In_{0.5}N$, Revista Colombiana de Física, [en línea]. 39(2), pp. 347-350, 2007. Disponible en: http://www.revcolfis.org/publicaciones/vol39_2/resumenes/3902347.html

[11] Abdel Rahim-Garzón, G.P. y Rodríguez-Martínez, J.A., Evolución de las propiedades estructurales y electrónicas en la transición de fase wurtzita-NaCl para el compuesto YIn_3N_4, Revista Colombiana de Física, [en línea]. 39(2), pp. 531-534, 2007. Disponible en: http://www.revcolfis.org/publicaciones/vol39_2/resumenes/3902531.html

[12] Abdel Rahim Garzón, G.P, y Rodríguez M.J.A., YInN: nueva perspectiva. Estudio de sus propiedades estructurales y electrónicas desde primeros principios, Tecnura, 8(16), pp. 4-14, 2005. DOI: 10.14483/22487638.6206

[13] Zoita, C.N., Braic, M. and Braic, V., Structural, optical and electronic properties of $In_{1-x}Y_xN$ thin films, Dig, J. Nanomater Biostructures, [online]. 6(4), pp. 1877-1886, 2011. Available at: https://citeseerx.ist.psu.edu/viewdoc/download?doi=10.1.1.1078.1195&rep=rep1&type=pdf

[14] Blaha, P., Schwarz, K., Madsen, G., Kvasnicka, D. and Luitz, J., WIEN2k, an augmented plane wave plus local orbitals program for calculating crystal properties, [online]. 2009. Available at: https://euler.phys.cmu.edu/cluster/WIEN2k/usersguide.pdf

[15] Perdew, J.P., Burke, K. and Ernzerhof, M., Generalized Gradient approximation, Phys. Rev. Lett, 77(8), pp. 3865-3868, 1996. DOI: DOI: 10.1016/j.spmi.2014.07.009.

[16] Cherchab, Y., Azzouz, M., González-Hernández, R. and Talbi, K., First-principles prediction of the structural and electronic properties of $Ga_xY_{1-x}N$ compounds, Computational Materials Science, 95, pp. 509-516, 2014. DOI: 10.1016/j.commatsci.2014.08.021.

[17] Talbi, K., Cherchab, Y. and Sekkal, N., Structural and electronic

properties of ScYN alloys and superlattices. The European Physical Journal Applied Physics, 58(3), art. 30103, 2012. DOI: 10.1051/epjap/2012110307

[18] Scharoch, P., Winiarski, M.J. and Polak, M.P., Ab initio study of $In_xGa_{1-x}N$ performance of the alchemical mixing approximation, Computational Materials Science, 81, pp. 358-365, 2014, DOI: 10.1016/j.commatsci.2013.08.047

[19] Gorczyca, I., Kaminska, A., Staszczak, G., Czernecki, R., Lepkowski, S.P., Suski, T., Schenk, H.P.D., Glauser, M., Butté, R., Carlin, J.-F. et al., Anomalous composition dependence of the band gap pressure coefficients in In-containing nitride semiconductors, Phys. Rev. B, [online]. 81, art. 235206, 2010. Available at: https://link.aps.org/doi/10.1103/PhysRevB.81.235206

[20] Osamura, K., Naka, S. and Murakami, Y., Preparation and optical properties of Ga1−xInxN thin films, Journal of Applied Physics 46, pp. 343, 1975. DOI: 10.1063/1.322064

[21] Gorczyca, I., Plesiewicz, J., Dmowski, L., Suski, T., Christensen, N.E., Svane, A., Gallinat, C.S., Koblmueller, G. and Speck. J.S., Electronic structure and effective masses of InN under pressure, J. Appl. Phys, 104, art. 013704, 2008. DOI: 10.1063/1.2953094

[22] Murnaghan, F.D., The compressibility of media under extreme pressures, Proc. Natl. Acad. Sci. U.S.A., 30(9), pp. 244-247 1944. 5390. DOI: 10.1073/pnas.30.9.244.

G.P. Abdel Rahim-Garzón, received the BSc. in Physics from the Universidad Distrital Fracisco José de Caldas in 1998, the MSc. in Physics in 2006, and the PhD in Engineering 2017, from the Universidad Nacional de Colombia and graduated with meritorious mention, Bogotá, Colombia. From 2005 to 2021, her worked is into new materials and the structural and electronic properties of materials, as well as surface physics of semiconductors. her is a full professor the Physics, Facultad Tecnológica, Universidad Distrital Francisco José de Caldas, Bogotá, Colombia. His research interests include: studies electronic and structural properties of materials, as well as surface physics of semiconductors, using the method of Density Functional Theory (DFT).
ORCID: 0000-0002-8620-7023

J.A. Rodríguez-Martínez, received the BSc. in Physics in 1981. MSc in Physics in 1989, and the PhD in Physics Science 1999, all of them from the Universidad Nacional de Colombia at Bogotá. Posdoctoral research position at Universidad Nacional Autónoma de México (UNAM) 2000 – 2001. He has been professor at Physics Dept., Universidad Nacional de Colombia, at Bogotá since 1987, and since 2010 he is titular professor. His main research in theoretical physics is oriented to condensed matter specially in surface physics by means of the computational methods based on DFT (Density Functional Theory). He has published more than 80 researchs in international physics journals, as Phys. Rev. B, Acta Crystallographica: Section E Journal of Magnetism and Magnetic Materials, Applied Surface Science, Materials Letters and others. About more 100 physics papers in scientific journals of Colombia, too.
ORCID: 0000-0001-7554-4422
Scopus Author ID: 7404697377

M.G. Moreno-Armenta, received the BSc in Biopharmacy Chemistry in 1976 from the Universidad Nacional Autónoma de México, the MSc. in Chemistry in 1994 from Instituto Tecnologico de Tijuana, and the PhD in Physics of Materials in 2000, from the Centro de Investigación Científica y de Educación Superior de Ensenada. Her research interests include: materials electronic structure calculations by first principles mainly of transition metals nitrides, oxides and carbides.
ORCID: 0000-0002-8040-0615

M.J. Espitia-R., received the BSc. in Physicist in 1999 from the Universidad de Córdoba, Colombia; the MSc. in Physical Science in 2008 and PhD. in Physical Sciences in 2016, all of them from the Universidad Nacional de Colombia, Bogotá, Colombia. From 1999 to 2004, he worked as a professor in the Physical Department, Universidad de Córdoba, Montería, Colombia. Since 2005 to day, he is a full associate professor in the Universidad Distrital Francisco José de Caldas, Bogotá, Colombia. His research interests include: simulation, computational calculation of new materials.
ORCID: 0000-0001-9903-4224